Available online at www.sciencedirect.com
SCIENCE DIRECT®
Bioorganic & Medicinal Chemistry 12 (2004) 2965–2972
Bioorganic & Medicinal Chemistry

Slow-binding inhibition of 2-keto-3-deoxy-6-phosphogluconate (KDPG) aldolase

Rémi Braga,[a] Laurence Hecquet[b] and Casimir Blonski[a,*]

[a]*Université Paul Sabatier, LSPCMIB, UMR 5068, Groupe de Chimie Organique Biologique, Bât IIR1, 118 Route de Narbonne, 31062 Toulouse Cedex 4, France*

[b]*Université Blaise Pascal, Laboratoire SEESIB, UMR 6504, 24, avenue des Landais, Campus des Cézeaux, 63177 Aubière Cedex, France*

Received 28 October 2003; accepted 16 March 2004
Available online 21 April 2004

Abstract—2-Keto-3-deoxy-6-phosphogluconate (KDPG) aldolase is a key enzyme in the Entner–Doudoroff pathway of bacteria. It catalyzes the reversible production of KDPG from pyruvate and D-glyceraldehyde 3-phosphate through a class I Schiff base mechanism. On the basis of aldolase mechanistic pathway, various pyruvate analogues bearing β-diketo structures were designed and synthesized as potential inhibitors. Their capacity to inhibit aldolase catalyzed reaction by forming stabilized iminium ion or conjugated enamine were investigated by enzymatic kinetics and UV–vis difference spectroscopy. Depending of the substituent R (methyl or aromatic ring), a competitive or a slow-binding inhibition takes place. These results were examined on the basis of the three-dimensional structure of the enzyme.

1. Introduction

Aldolases are subject of continuous interest owing to their central place in catalyzing carbon–carbon bond formation (or cleavage) in living organisms. 2-Keto-3-deoxy-6-phosphogluconate (KDPG) aldolase (E.C. 4.1.2.14) is a key enzyme in the Entner–Doudoroff pathway of bacteria.[1] It catalyzes the reversible production of KDPG from pyruvate and D-glyceraldehyde 3-phosphate (D-GAP) through a class I Schiff base mechanism.[2,3] The aldol condensation proceeds by several ordered steps (Scheme 1): iminium ion (or Schiff base) formation between the carbonyl of pyruvate and the ε-amino group of essential Lys residue (Lys 133 for the enzyme from *E. coli*);[4] (ii) enamine formation after proton abstraction at C_3 in the iminium ion; (iii) enamine reaction with the carbonyl of D-GAP to form a new C–C bond and a second Schiff base; and (iv) hydrolysis of the latter iminium ion leading to KDPG with a *S*-configuration at C_4 and free enzyme. This enzyme displays considerable substrate tolerance and appears as an useful catalyst for stereocontrolled carbon–carbon bond formation between pyruvate and a range of unnatural aldehydes.[5–7]

It has been shown that the accumulation of KDPG in bacteria is correlated with an immediate and significant decrease in growth.[8] This suggests that KDPG aldolase can be considered as a target for the development of new bacteriostatic or bactericidal drugs. With the exception of bromopyruvic acid[9] and fluorodinitrobenzene,[4,10] few inhibitors of KDPG aldolase have been developed to date, despite interest in such compounds. On the basis of the aldolase mechanistic pathway (Scheme 1), we considered the possibility of obtaining slow-binding inhibitions of this enzyme through the stabilization of reaction intermediates (iminium ion or enamine) within the enzyme by the use of pyruvate analogues bearing a β-dicarbonyl structure.[11] The expected reaction where occurs the formation of iminium ion and conjugated enamine is shown in Scheme 2. The stabilization of these intermediates is possible through hydrogen bonding and equilibrium between several structures.

In the present paper, we describe the synthesis of seven pyruvate analogues bearing such a structure (Scheme 3) and the mechanisms by which these compounds inhibit KDPG aldolase from *E. coli*. The mode of interaction of these compounds with aldolase was examined by enzyme kinetics and UV–vis difference spectroscopy.

* Corresponding author. Tel.: +335-61-55-64-86; fax: +335-61-55-60-11; e-mail: blonski@cict.fr

0968-0896/$ - see front matter © 2004 Elsevier Ltd. All rights reserved.
doi:10.1016/j.bmc.2004.03.039

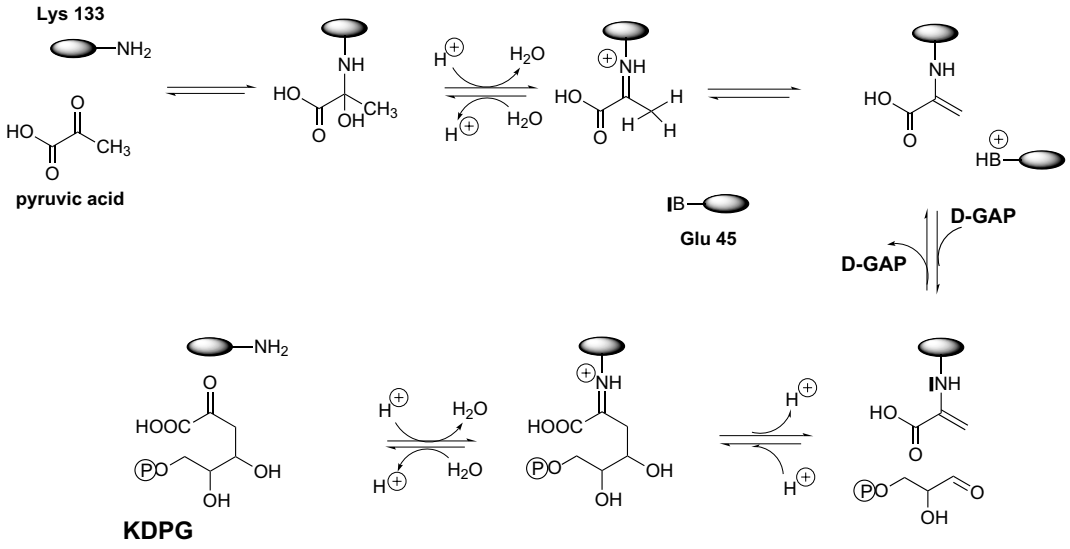

Scheme 1. Reaction catalyzed by KDPG aldolase and mechanistic pathway.

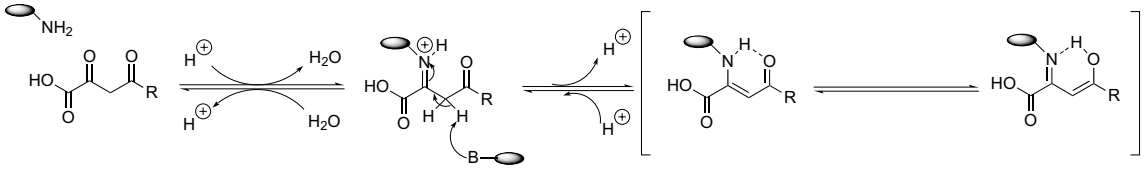

Scheme 2. Expected mechanistic pathway for KDPG aldolase inhibition by synthesized compounds.

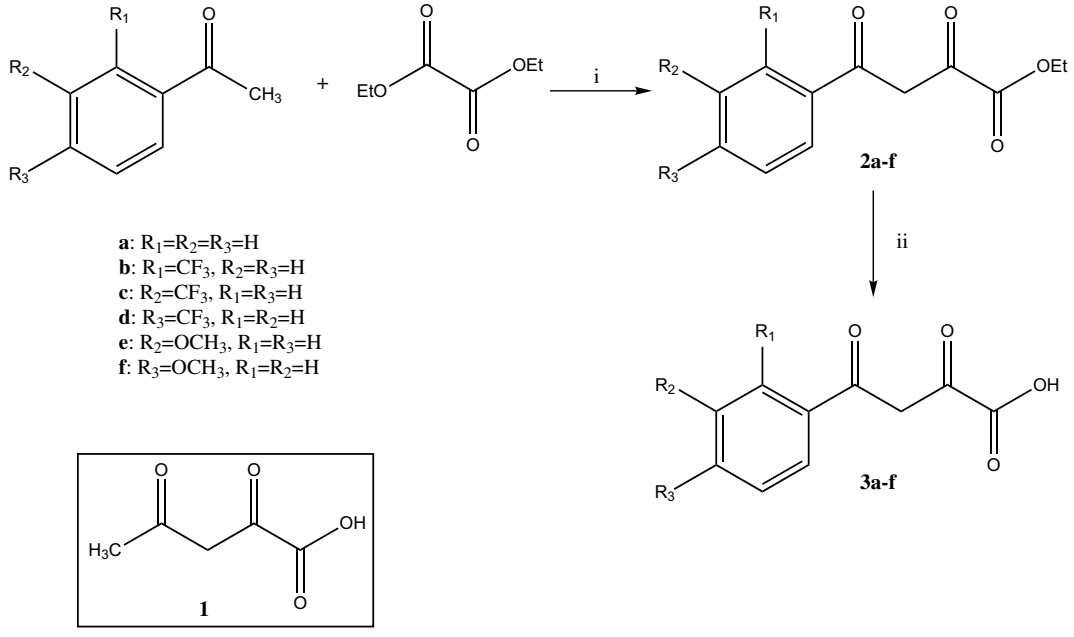

a: $R_1=R_2=R_3=H$
b: $R_1=CF_3$, $R_2=R_3=H$
c: $R_2=CF_3$, $R_1=R_3=H$
d: $R_3=CF_3$, $R_1=R_2=H$
e: $R_2=OCH_3$, $R_1=R_3=H$
f: $R_3=OCH_3$, $R_1=R_2=H$

Scheme 3. Synthetic scheme for synthesized compounds. (i) NaH; (ii) NaOH, H_2SO_4. Surrounded is indicated the structure of compound **1**.

2. Results

2.1. Synthesis

The β-diketo structure of compounds **2a**–**f** is generated by Claisen condensation of the appropriate methyl-ketone with diethyl oxalate in the presence of sodium hydride in refluxing toluene.[12] Diketoesters **2a**–**f** are then converted to the expected pyruvic acid analogues **3a**–**f** (Scheme 3). Acetylpyruvic acid **1** is obtained starting from the commercially available ethyl ester derivative in the same way.[13]

2.2. Enzymatic inhibition studies

2.2.1. Competitive inhibition of aldolase from *E. coli* by acetylpyruvic acid 1. KDPG aldolase activity was competitively inhibited in the presence of compound **1**, with K_i value of $250 \pm 20\,\mu M$. The Michaelis constant (K_m) determined for KDPG as substrate was $60 \pm 3\,\mu M$ (not shown).

2.2.2. Time-dependent inhibitions of aldolase by compounds 3a–f. Incubation of aldolase with compound **3a–f** resulted in a first-order rate loss of enzyme activity (as an example, Fig. 1 shows the results obtained with compound **3a**). The enzymatic activity is slowly but fully restored by the addition of saturating concentration (10 mM) of substrate pyruvate to the enzyme–inhibitor complex solutions (data not shown). This result is consistent with an inhibition occurring at the active site of the enzyme.

The time-dependent reversible inhibition observed (Fig. 1) and reversion by addition of excess of substrate suggest that compounds **3a–f** behave as slow-binding inhibitors of aldolase.[14] The analysis of the extent of inhibition (as an example, Fig. 2 shows the result obtained with compound **3a**) are consistent with a slow equilibrium formation between the enzyme, the inhibitor and the enzyme–inhibitor complex (see Eq. 1 in the Experimental section). This allows to determine the inhibition constant values, which are indicated in Table 1.

2.3. UV–vis difference spectroscopy

2.3.1. Interactions of compounds 3a–f with aldolase. The interactions of aldolase (10 μM subunits) with compounds **3a–f** (25–500 μM) resulted in UV–vis difference spectra characterized by the presence of isosbestic points, which indicates that there was no accumulation of intermediates nor side reactions. As an example, Figure 3 shows spectra obtained with compound **3a**.

The reactions of compound **3a–f** with the lysine residue of aldolase was modelled through the reaction of **3a–f** (250 μM) with aminocaproic acid (50 mM).[15,16] The

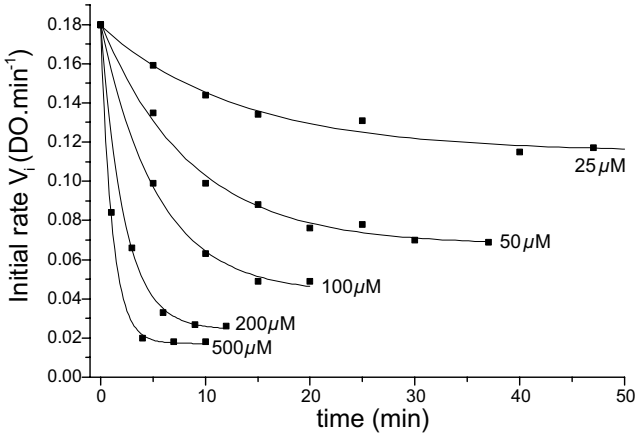

Figure 1. Time-dependent inhibition of aldolase by compound **3a**. Native recombinant aldolase ($0.2\,mg\,mL^{-1}$) was incubated in the presence of compound **3a** at the indicated concentration in TEA buffer (1 mL final volume). Aliquots were analyzed at various times for enzymatic activity (see the Experimental section). In control performed without inhibitor, no inhibition was observed.

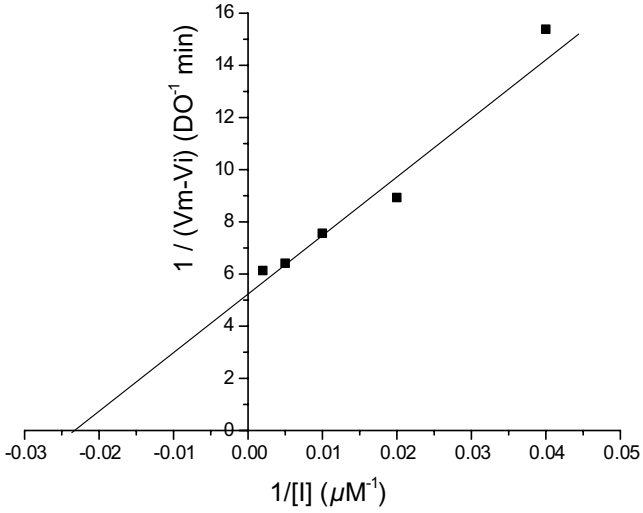

Figure 2. Compound **3a** as slow-binding aldolase inhibitor. Residual activity values at equilibrium were obtained from Figure 1. Data points are experimental, and the line represents the best fit of the data to Eq. 1. The K_i^* value determined was $70 \pm 10\,\mu M$.

Table 1. Dissociation constant values (K_i^*) describing the interaction of compounds **3a–f** with aldolase

Compounds	K_i^* (μM)
3a	70 ± 20
3b	40 ± 10
3c	30 ± 5
3d	380 ± 50
3e	75 ± 10
3f	180 ± 50

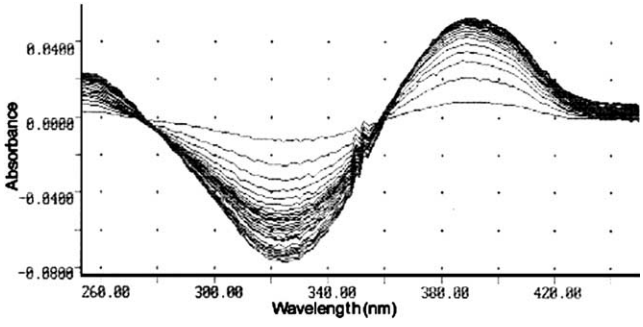

Figure 3. Interaction of aldolase with compound **3a**. UV–vis difference spectra of 10 μM aldolase subunits and 100 μM of compound **3a** in TEA buffer (1 mL final volume, pH 7.6) with time (interval of 2 min). Spectra are characterized by maximum at 390 nm, minimum at 318 nm and the presence of isosbestic points around 270 and 350 nm.

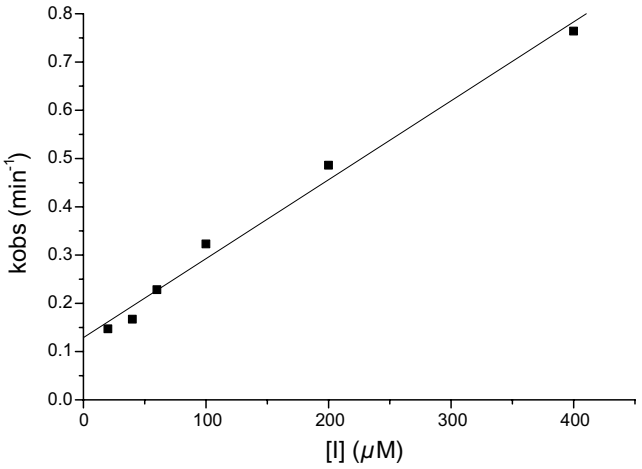

Figure 4. Determination of kinetic parameters for aldolase inhibition by compound **3a**. Data are experimental (provided by Fig. 3) and the line represent the best fit of the data to Eq. 2. The k_1 and k_{-1} values determined were $(2.61 \pm 0.03) \times 10^3\ M^{-1}\ min^{-1}$ and $0.109 \pm 0.009\ min^{-1}$, respectively. This allowed us to calculate K_i^* value, which was $70 \pm 10\ \mu M$.

same pattern of UV–vis difference spectra as for the reactions with aldolase was obtained (not shown).

Difference absorbance spectra such as shown in Figure 1 were consistent with a first-order process, which correlated with the loss of enzyme activity. Observed first-order rate constants present no saturation kinetics, a result consistent with the slow-binding scheme presented in the Experimental section and with the enzymatic inhibition studies. The kinetic parameter values associated with the EI* complex formation were obtained by fitting the data to Eq. 2 (as an example, Fig. 4 shows the result obtained with compound **3a**).

The resulting values are reported in Table 2 and the dissociation constant values (K_i^*) calculated from these results are in good agreement with those of Table 1, determined by an other approach.

Dissociation of the enzyme-**3a**–**f** complexes followed by UV–vis difference spectroscopy was observed at saturating concentration (10 mM) of substrate pyruvate (not shown). The pyruvate chase fully restored enzyme activity and the displacement of inhibitor from the enzymatic complex was characterized by first-order rate constants (k_{-1} values) in good agreement with those determined by the other method (Table 2).

3. Discussion

As a first remark, we underline the simple and efficient route that the Claisen reaction represents for the introduction of the β-diketo frame present in all inhibitors used in this work.

Second, the results obtained with compound **1**, which behaves as a competitive inhibitor, indicate that this frame is recognized by the enzyme: the extension of the carbon chain of two more carbon atoms does not prevent the recognition by the enzyme, although there is a loss of affinity from the substrate to compound **1** by a factor of 4.

Then, the replacement of the methyl group in **1** by an aromatic substituent in the series **3a**–**f** changes the inhibition, which becomes time dependent. The analysis of the interactions between the enzyme and this set of compounds is made by two independent approaches:

- by inhibition kinetics: results shown in Figure 2, the reversion of inhibition by adding an excess of substrate, both evidence a slow-binding process, the kinetic parameters of which can be determined. As a matter of fact, compounds **3b** and **3c** exhibit K_i^* values, clearly lower than K_m;
- by following in UV–vis difference spectroscopy the formation of the complex between an inhibitor of the **3a**–**f** series and the enzyme; the significant absorbance and the parallel with the reference reaction observed with aminocaproic acid indicate the formation of a stabilized intermediate, compatible with the proposed Scheme 2 and in agreement with the observed time-dependent kinetics. Moreover, the fair agreement obtained by the two independent methods between the two sets of K_i^* values, indicates that the enzyme inactivation and the formation of the complex are correlated. This point is also confirmed by the good agreement on the k_{-1} values, obtained in the one hand by inhibition kinetics and on the other by the chase pulse experiment where the inhibitor is displaced from the complex by adding large amounts of substrate. As this complex has a significant absorbance, it is likely that not only the Schiff base formation but also the proton abstraction step occur within the enzyme for the substrate analogues. This point has to be confirmed by other methods, particularly site directed mutagenesis. This will be done when possible residues acting as proton abstractor are identified from the X-ray structure, presently in progress,

Table 2. Kinetic parameter values associated with aldolase inhibition by compounds **3a**–**f**, determined by UV–vis difference spectroscopy technique

	Kinetic parameters			
Compounds	$k_1 \times 10^3$ ($M^{-1}\ min^{-1}$)	k_{-1} (min^{-1})		K_i^* (μM)
3a	2.61 ± 0.03	0.109 ± 0.009	(0.123 ± 0.025)[a]	70 ± 10
3b	3.90 ± 0.05	0.023 ± 0.002	(0.062 ± 0.011)	10 ± 1
3c	1.20 ± 0.01	0.075 ± 0.005	(0.035 ± 0.005)	60 ± 10
3d	0.46 ± 0.07	0.207 ± 0.003	(0.137 ± 0.014)	450 ± 10
3e	1.20 ± 0.02	0.160 ± 0.070	(0.117 ± 0.006)	130 ± 60
3f	0.43 ± 0.01	0.250 ± 0.003	(0.106 ± 0.010)	580 ± 20

[a] Values in parentheses were determined by chase pulse experiments (see text).

of crystals of inhibitor **3b** and KDPG aldolase from *E. coli*. For now, we underlined the interest of the UV spectroscopic method, which leads to reliable results and is of particular interest to investigate complexes formed between effectors and enzymes even after they lost their catalytic activity, for instance mutants.

The next point is related to the substituent effect observed with inhibitors of the **3a**–**f** series: it can be noticed from Table 2 that the best K_i^* values are obtained with inhibitors bearing an electron withdrawing substituent at position *ortho* or *meta* (**3b** and **3c)**, whereas the reverse situation is observed with the electron releasing group present in **3e** and **3f**. To account for this, we considered the X-ray structure obtained with KDPG aldolase from *E. coli* where the substrate pyruvate has been trapped in the carbinolamine form.[17] This structure shows that an aromatic residue, namely phenyl-alanine 135 points towards the C_3 carbon (or methyl group) in pyruvate, position where the group Aryl–C(O) is linked. It is therefore conceivable that π–π interactions occur between Phe-135 and the aryl group in the inhibitor, the interaction being stronger between an electron rich and an electron depleted aromatic rings than between two rings of similar densities, as observed for instance in Meisenheimer complexes.[18] Along these lines, it can be understood that CF_3 as substituent on the ring leads to stronger inhibition than compounds **3e** or **3f** bearing the electron donating group CH_3O, the phenyl ring in Phe-135 being electron rich. Again, a better understanding of this situation will be obtained when the X-ray structure of the complex of *E. coli* KDPG aldolase-**3b** will be solved. This may allow also to introduce other substituents on the chain, possibly contributing to an improved affinity. For now, we present the access to a new class of KDPG aldolase inhibitors and a strategy to study and improve them.

4. Experimental

4.1. Enzymes and reagents

Pyruvic acid sodium salt, glycerol phosphate dehydrogenase, triose-phosphate isomerase and lactic dehydrogenase were purchased from Boehringer Mannheim. All other chemicals were purchased from Aldrich and were used without extra purification. KDPG aldolase from *E. coli* was kindly provided to us by Pr Sygusch (Montreal University). Substrate KDPG was prepared as described previously.[19]

4.2. Assay methods

Aldolase activity (25 units mg^{-1} at 25 °C) was measured by means of lactic dehydrogenase method in 1 mL of 0.1 M triethanolamine hydrochloride buffer (pH 7.6 and ionic strength 0.15), using KDPG (1 mM) as substrate as described elsewhere,[20] except for compound **1**, which was found to inhibit lactic dehydrogenase; aldolase activity in the presence of this compound was then measured by means of triose-phosphate isomerase/glycerol phosphate dehydrogenase as previously reported.[21] The protein concentration was estimated using the molecular absorbance at $\lambda = 280$ nm ($\varepsilon = 18,260\ L\ mol^{-1}\ cm^{-1}$, calculated by Schepartz Lab Biopolymer Calculator[22]). The subunit concentration was determined assuming a molecular weight of 67,000 for the trimeric aldolase.

4.3. Kinetic parameters and equilibrium constants values determination

The data were subjected to a linear least square fit to the appropriate equation using the Origin program.

4.4. Competitive inhibition study

The dissociation constant of the enzyme–inhibitor complex was determined by double reciprocal plots of initial velocities of aldolase (0.33 μg mL^{-1}) for KDPG and compound **1** concentrations in the range of 100–500 and 0–500 μM, respectively.

4.5. Inhibition study

Aldolase (0.2 mg mL^{-1} in 0.1 mL TEA buffer) was incubated in the presence of the compound under study (0.025–0.5 mM). The enzymatic activity was assayed as a function of time with 10 μL aliquots. Control experiments were run without inhibitor and all measurements were made in duplicate.

4.6. Equations

In this study, slow-binding inhibition[14] involves a slow equilibrium formation between the enzyme E, the inhibitor I and the enzyme–inhibitor complex EI* as shown below:

$$E + I \underset{k_{-1}}{\overset{k_1}{\rightleftharpoons}} EI^* \quad K_i = \frac{k_{-1}}{k_1}$$

K_i^* is the dissociation constant for the EI* complex.
Characterization of slow-binding inhibition: in the absence of substrate, the following two equations were used for the determination of the kinetic parameter values:

$$\frac{1}{V_m - V_i} = \frac{1}{V_m} + \frac{K_i^*}{V_m[I]} \quad (1)$$

$$k_{obs} = k_{-1} + k_1[I] \quad (2)$$

V_m and V_i represent, respectively, the residual enzymatic activity in the absence and in the presence of the inhibitor; the apparent first-order rate constants (k_{obs}) describing the formation of EI* parallel the increasing concentration of inhibitor ([I]).

4.7. UV–vis difference spectroscopy

Absorbance spectra were measured using a Cary 1E Varian spectrophotometer at constant 25 °C. The same TEA buffer as for enzymatic kinetic studies was utilized. Absorbance spectra were measured using a previously described method.[15,16] Absorption spectra were scanned between 250 and 450 nm and recorded as a function of time. Measurements were initiated by addition of the compound under study at various final concentrations to TEA buffer solutions containing a fixed concentration of aldolase (10 μM subunit). The measured absorption spectra of the enzyme complex recorded at timed intervals were corrected for absorption by buffer, compound under study and the enzyme alone. For the model study, absorption spectra were recorded at timed intervals and corrected for absorption by buffer, compounds and aminocaproic acid. Observed apparent first-order rate constants, k_{obs} were obtained for each assay by fitting the time-dependent absorption data against a first-order kinetic equation using the Origin program. The dissociation constant (K_i^*) and the rate constants k_1 and k_{-1} (corresponding to the formation and dissociation of the slow-binding aldolase–inhibitor complex, respectively), are derived from analysis of apparent rate constants using Eq. 2.

The first-order rate constant k_{-1} was also derived independently from absorbance data corresponding to the displacement of the inhibitor under study from the enzymic complex by 10 mM pyruvate.

4.8. Synthesis

NMR spectra were recorded in $CDCl_3$, CD_3OD, acetone-d_6 or DMSO-d_6 on Bruker AC200 and AC250 spectrometers. All chemical shifts (δ) are reported in parts per million (ppm) with respect to TMS for ^1H and ^{13}C spectra and trifluoroacetic acid for ^{19}F spectra as internal standard.

4.8.1. Acetylpyruvic acid (1). This compound was prepared as described previously,[13] starting form the ethyl ester derivative.

^1H NMR (250 MHz, $CDCl_3$): 6.46 (s, 1H), 2.28 (s, 3H). ^{13}C NMR (63 MHz, $CDCl_3$): 199.2, 167.6, 164.4, 101.8, 27.1.

The esters **2a**–**f** were prepared by Claisen condensation of diethyloxalate with the corresponding methyl ketone as previously reported.[23]

4.8.2. Ethyl 2,4-dioxo-4-phenylbutanoate (2a). To a mixture of acetophenone (2 g, 16.6 mmol) and diethyloxalate (3.4 mL, 25.0 mmol) in 50 mL of anhydrous toluene was added sodium hydride (0.8 g, 33.3 mmol). The resulting mixture was stirred at 80 °C for 2 h; the solvent was evaporated under vacuo, the crude mixture placed in 50 mL of ethyl acetate and washed once with 25 mL of water. The organic layer was dried over sodium sulfate and evaporated in vacuo. The remaining product was purified by silica chromatography ($CHCl_3$) to yield **2a** as a yellow oil (0.9 g, 25%). ^1H NMR (250 MHz, $CDCl_3$): 7.95 (d, 2H, $^3J_{H-H} = 8$ Hz), 7.56–7.36 (m, 3H), 7.01 (s, 1H), 4.30 (q, 2H, $^3J_{H-H} = 7$ Hz),1.34 (t, 3H, $^3J_{H-H} = 7$ Hz). ^{13}C NMR (63 MHz, $CDCl_3$): 190.7, 169.7, 139.5, 134.8, 133.7, 128.8, 127.8, 97.9, 62.5, 14.1.

4.8.3. Ethyl 2,4-dioxo-4-[2-(trifluoromethyl)phenyl]butanoate (2b). The compound was prepared by following the same procedure as **2a**, using (2-trifluoromethyl)acetophenone (1 g, 5.3 mmol), diethyloxalate (1.1 mL, 8.0 mmol) and sodium hydride (0.3 g, 10.6 mmol). The remaining product was purified by silica chromatography (toluene/AcOEt 7:3–1:1) to yield **2b** as an orange oil (0.4 g, 23%). ^{19}F NMR (188 MHz, $CDCl_3$): 17.39. ^1H NMR (250 MHz, $CDCl_3$): 7.61 (d, 1H, $^3J_{H-H} = 7$ Hz), 7.38 (s, 2H), 7.25 (m, 1H), 6.21 (s, 1H), 4.12 (q, 2H, $^3J_{H-H} = 7$ Hz), 1.21 (t, 3H, $^3J_{H-H} = 7$ Hz). ^{13}C NMR (63 MHz, $CDCl_3$): 192.3, 169.4, 166.9, 142.0, 125.4 (q, $^3J_{C-F} = 250$ Hz), 130.4, 129.8, 127.4, 126.2, 99.0, 62.0, 13.8.

4.8.4. Ethyl 2,4-dioxo-4-[3-(trifluoromethyl)phenyl]butanoate (2c). The same procedure as for **2b** was followed, using (3-trifluoromethyl)acetophenone as starting material. The remaining residue was purified by silica chromatography (toluene to toluene/AcOEt 8:2) to yield **2c** as an orange oil (0.2 g, 12%). ^{19}F NMR (188 MHz, $CDCl_3$): 12.63. ^1H NMR (250 MHz, $CDCl_3$): 8.17 (s, 1H), 8.11 (d, 1H, $^3J_{H-H} = 8$ Hz), 7.80 (d, 1H, $^3J_{H-H} = 8$ Hz), 7.60 (t, 1H, $^3J_{H-H} = 8$ Hz), 7.04 (s, 1H), 4.36 (q, 2H, $^3J_{H-H} = 7$ Hz), 1.37 (t, 3H, $^3J_{H-H} = 7$ Hz). ^{13}C NMR (63 MHz, $CDCl_3$): 188.7, 170.7, 161.8, 131.5 (q, $^3J_{C-F} = 250$ Hz), 130.8, 129.9, 127.6, 124.3, 121.3, 120.2, 97.7, 62.7, 13.9.

4.8.5. Ethyl 2,4-dioxo-4-[4-(trifluoromethyl)phenyl]butanoate (2d). Reagents were used according to the same procedure as **2a**, using (4-trifluoromethyl)acetophenone (0.5 g, 2.7 mmol), diethyloxalate (0.6 mL, 4.0 mmol) and sodium hydride (0.2 g, 5.3 mmol). The product was purified by silica chromatography ($CHCl_3$ to $CHCl_3$/CH_3OH 9:1) to yield **2d** as an orange oil (0.3 g, 37%). ^{19}F NMR (188 MHz, $CDCl_3$): 12.4. ^1H NMR (250 MHz, $CDCl_3$): 8.09 and 7.72 (d, 4H, $^3J_{H-H} = 8$ Hz), 7.06 (s, 1H), 4.38 (q, 2H, $^3J_{H-H} = 7$ Hz), 1.26 (t, 3H, $^3J_{H-H} = 7$ Hz). ^{13}C NMR (63 MHz, $CDCl_3$): 188.5, 171.4, 162.9, 137.8, 132.5 (q, $^3J_{C-F} = 32$ Hz), 128.4, 125.9, 122.1, 97.9, 45.8, 14.1.

4.8.6. Ethyl 4-(3-methoxyphenyl)-2,4-dioxobutanoate (2e). (3-Methoxy)acetophenone (1 g, 6.7 mmol), diethyloxalate (2.0 mL, 10.0 mmol) and sodium hydride (0.3 g, 13.4 mmol) were utilized as described above. The crude product was purified by silica chromatography (CH_2Cl_2/n-C_6H_{12} 8:2) to yield **2e** as a colourless oil (0.8 g, 49%).

^{1}H NMR (250 MHz, acetone-d_6): 7.38 (t, 2H, $^3J_{H-H} = 8$ Hz), 7.27 (t, 1H, $^3J_{H-H} = 8$ Hz), 7.01 (d, 1H, $^3J_{H-H} = 8$ Hz), 6.90 (s, 1H), 4.24 (q, 2H, $^3J_{H-H} = 7$ Hz), 3.71 (s, 3H), 1.28 (t, 3H, $^3J_{H-H} = 7$ Hz). ^{13}C NMR (63 MHz, acetone-d_6): 190.6, 169.2, 162.0, 159.9, 155.2, 152.1, 149.5, 142.3, 112.2, 98.0, 62.4, 55.3, 14.0.

4.8.7. Ethyl 4-(4-methoxyphenyl)-2,4-dioxobutanoate (2f). The same procedure as for **2a** was followed, using (4-methoxy)acetophenone (1 g, 6.7 mmol), diethyloxalate (2.0 mL, 10.0 mmol) and sodium hydride (0.3 g, 13.4 mmol). The product was purified by silica chromatography (diethyl ether/petroleum ether 1:1) to yield **2f** as a colourless oil (0.4 g, 25%). ^{1}H NMR (250 MHz, $CDCl_3$): 7.82 (d, 2H, $^3J_{H-H} = 9$ Hz), 6.83 (d, 2H, $^3J_{H-H} = 9$ Hz), 6.88 (s, 1H), 4.27 (q, 2H, $^3J_{H-H} = 7$ Hz), 3.75 (s, 3H), 1.29 (t, 3H, $^3J_{H-H} = 7$ Hz). ^{13}C NMR (63 MHz, $CDCl_3$): 190.2, 167.9, 164.3, 162.3, 158.2, 154.3, 152.9, 150.1, 114.1, 97.6, 62.4, 55.5, 14.0.

4.8.8. 2,4-Dioxo-4-phenylbutanoic acid (3a). To a solution of **2a** (0.12 g, 0.51 mmol) in 5 mL of water was added 0.25 mL of sodium hydroxide 4 N, and the mixture was vigorously stirred at room temperature for 2 min. The solution was then acidified with H_2SO_4 6 N to pH 3, the crude product was extracted six times with 10 mL diethyl ether; the organic layers were pooled and the solvent evaporated in vacuo. The remaining product was crystallized (using CCl_4 as solvent) to yield **3a** as a yellow powder (0.10 g, 67%). ^{1}H NMR (250 MHz, $CDCl_3$): 8.02 (d, 2H, $^3J_{H-H} = 8$ Hz), 7.67–7.49 (m, 3H), 7.18 (s, 1H). ^{13}C NMR (63 MHz, $CDCl_3$): 187.3, 173.3, 163.5, 133.5, 134.1, 129.0, 127.9, 95.9. Anal. Calcd for $C_{10}H_8O_4$: C, 62.50; H, 4.20. Found: C, 62.35; H, 4.15. Mass spectrometry (FAB): 193 $[M+H]^+$.

4.8.9. 2,4-Dioxo-4-[2-(trifluoromethyl)phenyl]butanoic acid (3b). This compound was prepared from **2b** (0.34 g, 1.2 mmol) by following the same procedure as for **3a** using sodium hydroxide pellets (0.06 g, 2.4 mmol), except that the mixture was vigorously stirred at room temperature for half an hour. The crude product was then crystallized (CCl_4) to yield **3b** as a white powder (0.11 g, 36%). ^{19}F NMR (188 MHz, DMSO-d_6): 23.43. ^{1}H NMR (250 MHz, DMSO-d_6): 7.87–7.69 (m, 4H), 6.47 (s, 1H). ^{13} C NMR (63 MHz, DMSO-d_6): 185.4, 163.3, 137.2, 132.6, 126.5 (q, $^3J_{C-F} = 250$ Hz), 130.0, 129.2, 128.9, 128.7, 102.5. Anal. Calcd for $C_{11}H_7O_4F_3$: C, 50.78; H, 2.71. Found: C, 50.35; H, 2.61. Mass spectrometry (FAB): 261 $[M+H]^+$.

4.8.10. 2,4-Dioxo-4-[3-(trifluoromethyl)phenyl]butanoic acid (3c). By following the same procedure as for **3b**, compound **2c** (0.14 g, 0.5 mmol) yielded the expected compound **3c** as a white powder (0.05 g, 39%). ^{19}F NMR (188 MHz, $CDCl_3$): 12.65. ^{1}H NMR (250 MHz, $CDCl_3$): 8.25 (s, 1H), 8.17 (d, 1H, $^3J_{H-H} = 8$ Hz), 7.88 (d, 1H, $^3J_{H-H} = 8$ Hz), 7.67 (t, 1H, $^3J_{H-H} = 8$ Hz), 7.20 (s, 1H). ^{13}C NMR (63 MHz, $CDCl_3$): 186.3, 173.7, 162.4, 134.4, 131.5 (q, $^3J_{C-F} = 250$ Hz), 130.9, 127.8, 126.1, 124.7, 121.3, 96.4. Anal. Calcd for $C_{11}H_7O_4F_3$: C, 50.78; H, 2.71. Found: C, 50.38; H, 2.59. Mass spectrometry (FAB): 261 $[M+H]^+$.

4.8.11. 2,4-Dioxo-4-[4-(trifluoromethyl)phenyl]butanoic acid (3d). By following the same procedure as for **3b**, compound **2d** (0.29 g, 1.0 mmol) yielded the expected compound **3d** as a white powder (0.11 g, 44%). ^{19}F NMR (188 MHz, DMSO-d_6): 18.6. ^{1}H NMR (250 MHz, DMSO-d_6): 8.23 (d, 2H, $^3J_{H-H} = 8$ Hz), 7.90 (d, 2H, $^3J_{H-H} = 8$ Hz), 7.11 (s, 1H), 2.49 (m, 2H). ^{13}C NMR (63 MHz, DMSO-d_6): 187.8, 171.2, 162.9, 138.0, 132.5 (q, $^3J_{C-F} = 32$ Hz), 130.0, 125.8, 121.4, 98.2. Anal. Calcd for $C_{11}H_7O_4F_3$,H_2O: C, 47.49; H, 3.26. Found: C, 47.12; H, 3.08. Mass spectrometry (FAB): 261 $[M+H]^+$.

4.8.12. 4-(3-Methoxyphenyl)-2,4-dioxobutanoic acid (3e). This compound was prepared from **2e** (0.40 g, 1.6 mmol) by following the above procedure to yield the expected compound **3e** as a pink powder (0.20 g, 57%). ^{1}H NMR (250 MHz, CD_3OD): 7.68 (d, 1H, $^3J_{H-H} = 8$ Hz), 7.58 (s, 1H), 7.49 (t, 1H, $^3J_{H-H} = 8$ Hz), 7.26 (d, 1H, $^3J_{H-H} = 8$ Hz), 7.14 (s, 1H), 3.92 (s, 3H). ^{13}C NMR (63 MHz, CD_3OD): 191.3, 163.1, 161.0, 130.9, 130.8, 121.1, 120.9, 120.7, 120.0, 98.5, 55.8. Anal. Calcd for $C_{11}H_{10}O_5$: C, 59.46; H, 4.54. Found: C, 59.28; H, 4.34. Mass spectrometry (FAB): 223 $[M+H]^+$.

4.8.13. 4-(4-Methoxyphenyl)-2,4-dioxobutanoic acid (3f). This compound was prepared from **2f** (0.40 g, 1.6 mmol) by following the above procedure to yield **3f** as a red powder (0.22 g, 61%). ^{1}H NMR (250 MHz, acetone-d_6): 8.11 (d, 2H, $^3J_{H-H} = 8$ Hz), 7.13 (d, 2H, $^3J_{H-H} = 8$ Hz), 7.11 (s, 1H), 3.93 (s, 3H). ^{13}C NMR (63 MHz, acetone-d_6): 191.2, 165.4, 163.4, 131.1, 130.6, 125.4, 115.1, 97.9, 56.0. Anal. Calcd for $C_{11}H_{10}O_5$: C, 59.46; H, 4.54. Found: C, 59.44; H, 4.54. Mass spectrometry (FAB): 223 $[M+H]^+$.

Acknowledgements

We are thankful to J. Sygusch for providing KDPG aldolase. We also acknowledge Y. Boublik, M. Bardet and M. Sancelme for technical assistance.

References and notes

1. Conway, T. *FEMS Microbiol. Rev.* **1992**, *9*, 1.
2. Meloche, H. P.; Wood, W. A. *J. Biol. Chem.* **1964**, *239*, 3511.
3. Grazi, E.; Meloche, H. P.; Martinez, G.; Wood, W. A.; Horecker, B. L. *Biochem. Biophys. Res. Commun.* **1963**, *10*, 4.
4. Ingram, J. M.; Wood, W. A. *J. Biol. Chem.* **1965**, *240*, 4146.
5. Allen, S. T.; Heintzelman, G. R.; Toone, E. J. *J. Org. Chem.* **1992**, *57*, 426.

6. Machajewski, T. D.; Wong, C. H. *Angew. Chem., Int. Ed.* **2000**, *39*, 1352.
7. Shelton, M. C.; Cotterill, I. C.; Novak, S. T. A.; Poonawala, R. M.; Sudarshan, S.; Toone, E. J. *J. Am. Chem. Soc.* **1996**, *118*, 2117.
8. Fuhrman, L. K.; Wanken, A.; Nickerson, K. W.; Conway, T. *FEMS Microbiol. Lett.* **1998**, *159*, 261.
9. Meloche, H. P. *Biochemistry* **1967**, *6*, 2273.
10. Barran, L. R.; Wood, W. A. *J. Biol. Chem.* **1971**, *246*, 4028.
11. Gefflaut, T.; Blonski, C.; Perie, J. *Bioorg. Med. Chem.* **1996**, *4*, 2043.
12. Marvel, C. S.; Dreger, E. E.. In: *Org. Synth. Coll.*; Wiley: New York, 1941; Vol. I, p 238.
13. Lehninger, A. L.; Witzemann, E. J. *J. Am. Chem. Soc.* **1942**, *64*, 874.
14. Morrison, J. F.; Walsh, C. T. *Adv. Enzyme Relat. Areas Mol. Biol.* **1987**, *61*, 201.
15. Santi, D. V.; Ouyang, T. M.; Tan, A. K.; Gregory, D. H.; Scanlan, T.; Carreras, C. W. *Biochemistry* **1993**, *32*, 11819.
16. Blonski, C.; De Moissac, D.; Perie, J.; Sygusch, J. *Biochem. J.* **1997**, *323*, 71.
17. Allard, J.; Grochulski, P.; Sygusch, J. *Proc. Natl. Acad. Sci. U.S.A.* **2001**, *98*, 3679.
18. Jones, J. B.; Sih, C. J.; Perlman, D. In *Applications of Biochemical Systems in Organic Chemistry—Part II*; Wiley: New York, 1976; Vol. X.
19. O'Connell, E. L.; Meloche, H. P. *Methods Enzymol.* **1982**, *89*, 98.
20. Meloche, H. P.; Ingram, J. M.; Wood, W. A. *Methods Enzymol.* **1967**, *9*, 520.
21. Rose, I. A.; O'Connell, E. L.; Mehler, A. H. *J. Biol. Chem.* **1965**, *240*, 1758.
22. Schepartz Lab Biopolymer Calculator, found in http://paris.chem.yale.edu/extinct.html.
23. Pei, Y.; Wickham, B. O. S. *Tetrahedron Lett.* **1993**, *34*, 7509.